OBJECT DETECTION UTILIZING A LINEAR RETRIEVAL ALGORITHM FOR THERMAL INFRARED IMAGERY*

Michael S. Ramsey
Department of Geology
Arizona State University
Tempe, Arizona USA

ABSTRACT

Thermal infrared (TIR) spectroscopy and remote sensing have been proven to be extremely valuable tools for mineralogic discrimination. One technique for sub-pixel detection and data reduction, known as a spectral retrieval or unmixing algorithm, will prove useful in the analysis of data from scheduled TIR orbital instruments. This study represents the first quantitative attempt to identify the limits of the model, specifically concentrating on the TIR. The algorithm was written and applied to laboratory data, testing the effects of particle size, noise, and multiple end-members, then adapted to operate on airborne Thermal Infrared Multispectral Scanner data of the Kelso Dunes, CA, Meteor Crater, AZ, and Medicine Lake Volcano, CA. Results indicate that linear spectral unmixing can produce accurate end-member detection to within an average of 5%. In addition, the effects of vitrification and textural variations were modeled. The ability to predict mineral or rock abundances becomes extremely useful in tracking sediment transport, desertification, and potential hazard assessment in remote volcanic regions.

1.0 INTRODUCTION

The fundamental goal of remote sensing measurements, whether in the laboratory or from space, is to determine the physical characteristics of the object under study. For measurements of the Earth's surface and depending on the wavelength region examined, these properties can include factors such as roughness, mineralogy, temperature, particle size, and elemental abundance. These wavelength regions are limited to windows of high atmospheric transmission. As technology, interest, and the speed of acquiring this information have increased, the resulting larger data volumes have necessitated faster and more accurate processing tools (Adams et al., 1989).

One such data reduction technique is linear deconvolution, which has been used in the past for a variety of scientific problems involving mixing analyses. Recently, several workers have adapted it to both the visible/near-infrared (VNIR), and to a lesser extent, the thermal infrared (TIR) portions of the EM spectrum (Johnson, et al., 1983; Gillespie, 1992; Thomson and Salisbury, 1993). The fundamental principle of spectral mixture analysis is that the emitted or reflected energy from a multimineralic surface is a linear combination of the energy radiated from each component in proportion to its areal percentage. Using the spectra of the pure end-members, mixed spectra can then be deconvolved through a least-squares fit resulting in a percentage of each input end-member plus several measures of the model quality. Unmixing provides a relatively straight forward and computationally quick method of assessing the mineral assemblages of the surface thereby reducing hyperspectral data sets to a minimum informational volume. In addition, the products of such an analysis (areal percentage, end-members present, and model error) are easier to interpret, especially when translated into an image format, than are thermal radiance values or arbitrarily classified pixels. However, after several years of use producing very good qualitative results, the need has arisen for a quantitative investigation into the limits and applicability of such a technique to thermal emission spectra emphasizing non-ideal input conditions and evaluating the associated errors.

The theory of linear mixing of end-member radiant energy is not new. Early, pioneering work into laboratory reflectance and thermal emission spectroscopy led Lyon (1964) to suggest the possibility of linearity. Multispectral data returned from lunar missions, and over a decade later from Mars, were analyzed by a similar approach (Singer and McCord, 1979; Adams et al., 1986). These studies, concentrated on the VNIR region, could only distinguish

* Presented at the Second International Airborne Remote Sensing Conference and Exhibition, San Francisco, California, 24-27 June 1996.

albedo patterns and broad soil classifications due to the low spectral resolution of the instruments available and the wavelength region sampled. Recently, the 7 VNIR spectral bands of the Thematic Mapper (TM) instrument aboard Landsat have made it possible to distinguish vegetation types and monitor deforestation (Adams et al., 1995) and examine eolian sand sea dynamics (Blount et al., 1990) using a linear deconvolution method. The use, viability, and potential of thermal infrared remote sensing for geological applications have been shown by other authors (Kahle and Goetz, 1983; Crowley and Hook, 1996).

Today, the TM and the Advanced Very High Resolution Radiometer (AVHRR) instruments provide the only spaceborne coverage in the thermal infrared. These instruments acquire repetitive data over much of the globe, however are hindered by low spatial and spectral resolution. For example, TM has 120 m per pixel spatial resolution with only one broadband channel between 10.5 μm and 12.5 μm; whereas AVHRR's resolution is 1 km per pixel, but is designed with two broadband channels spanning the thermal atmospheric window. With NASA's airborne Thermal Infrared Multispectral Scanner (TIMS) high spatial resolution, multispectral TIR data became available (Kahle and Goetz, 1983). The TIMS instrument is a thermal infrared imaging device utilizing six spectral bands from 8 μm to 12 μm (Palluconi and Meeks, 1985). The resolution of individual TIMS pixels can vary as a function of the aircraft's altitude, typically having a range of 5-10 m per pixel for most geologic investigations. This produces data that are over an order of magnitude more detailed than that of the Thematic Mapper. The TIMS is also serving as simulator for the future, Advanced Spaceborne Thermal Emission and Reflectance Radiometer (ASTER). The ASTER instrument, scheduled fore launch in 1998 aboard the first Earth Observing Satellite, will have 14 channels, 5 of which will span the thermal infrared region (Kahle et al., 1991). With a resolution of 90 m per pixel, the thermal portion of the ASTER data products will exceed the spatial resolution of current satellite data.

Despite the simpler physics involved with TIR spectroscopy and remote sensing, there has been a noticeable lack of past research in the area of unmixing. Gillespie (1992) applied an unmixing model to airborne TIMS imagery of Death Valley, California and was able to discriminate 4 end-members -- vegetation, quartzite, basalt, and "virtual cold". There was no attempt to field-verify the model end-members, however. The unmixing technique used in this study deconvolves the data in radiance space, rather than emissivity, resulting in one less degree of freedom, and thereby producing the need for a temperature influenced "virtual cold" end-member. Unmixing in emissivity space after temperature separation is desirable, however, since it provides for direct and meaningful comparison with laboratory spectra. It also produces a sample or pixel brightness temperature, and allows one more degree of freedom for the model and hence, the addition of one more possible end-member. Another significant mixing study in the TIR is that of Thomson and Salisbury (1993), who used high resolution reflection spectroscopy to study several different mixtures at unimodal size fractions. No attempt was made to apply a retrieval approach to the data, however. Rather, a forward analysis of comparing the physically mixed spectrum to the numerically mixed one, showed agreements to within 5% and prompted the authors to state the assumption of linear mixing in thermal infrared is valid.

The need for research on thermal emission data becomes important for several reasons. Most noticeably is that most geologically relevant minerals have diagnostic features in this region and their mixtures are decipherable without the invocation of higher level radiative transfer theory. Further, all thermal remote sensing instruments acquire emitted, rather than reflected, energy from the surface. Interpretation of their data will benefit from laboratory studies and well-documented spectral libraries. In the next several years, for instance, the high spectral resolution Thermal Emission Spectrometer (TES) will be returning data from Mars (Christensen et al., 1992), and the ASTER will acquire global, 5-channel image data of Earth for the first time.

It is the purpose of this research to expand upon thermal emission spectroscopy in the linear unmixing realm with specific emphasis towards remote sensing applications. The retrieval algorithm, designed and coded for thermal emission spectra, operates in the reverse sense, utilizing a Chi-squared minimization technique to perform a least-squares fit of the composite spectrum. The predicted percentages are then compared to the actual mineral end-member percentage within the mixture, and the root-mean-squared (RMS) error used to assess the quality of the data fit. For the laboratory analysis, mineral mixtures of various numbers and particle sizes were constructed, and emission spectra acquired. In addition, results were examined after an increase of random noise and several blind end-member input cases. In the case of the image data, several different sites were chosen to test the model under a variety of surface and mixing conditions. Image and laboratory derived end-members were used for this phase, comparing the model results to petrographic and spectroscopic analysis of field samples. A graph of the various input conditions and model permutations used for this study is shown in Figure 1.

	LABORATORY							IMAGERY			
COND / #NM	PHYSICAL MIXING	NUMERICAL MIXING (BLIND)	PART. SIZE EFFECTS (SAME NM)	PART. SIZE EFFECTS (DIFF NM)	NOISE EFFECTS	REPRO. EFFECTS	TOTAL	LAB-DER. ENDMBERS (USER-DEF)	LAB-DER. ENDMBERS (BLIND)	IMAGE-DERIVED ENDMBERS	RESOLUTION EFFECTS
2	●		●	●			50				
3	●				●		8	●		●	●
4	●					●	11	●	●		
5		●			●		12				
10		●			●		4				
15		●					1				

Figure 1. Model trial matrix used in this study for both laboratory and thermal infrared image data. Each marked box represents a different input effect tested on a given end-member suite of mineral mixtures.

2.0 THEORY

2.1 THERMAL INFRARED EMISSION FROM NATURAL SURFACES

The thermal energy, or radiance, emitted at any given wavelength is a function of both the temperature of the object as well as its emissivity. The radiance, temperature and emissivity are related through the Planck equation,

$$L_{(\lambda,T)} = \varepsilon_\lambda B_{(\lambda,T)} = \varepsilon_\lambda \left\{ \frac{C_1 \lambda^{-5}}{\left[\exp(C_2/\lambda T) - 1\right]} \right\} \quad (1)$$

where, $C_1 = 3.74 \times 10^{-16}$ W-m^2 and $C_2 = 0.0144$ m-K. An object with an emissivity value equal to unity radiates a featureless spectrum at all wavelengths and is defined as a blackbody emitter. Solving equation (1) for the emissivity term produces the spectrum of the unknown sample, which is the ratio of its calibrated radiance to that of a blackbody at the same temperature (assuming a known sample emissivity at some wavelength). Most materials have spectra with emissivity values less than one at discrete wavelengths that are caused by the vibrational stretching and bending frequencies of the chemical bonds (Figure 2). Emissivity lows, commonly called absorption bands, are characteristic signatures of the object being analyzed. All silicate minerals contain a characteristically large feature between 9 and 12 µm, called the reststrahlen band (Salisbury and Walter, 1989). Caused by stretching of the silicon-oxygen bond, this band shifts from 9 to 11 µm (lower frequencies) with increasing silica depolymerization.

Because of the higher absorption coefficients of most minerals in the thermal infrared, photon/matter interaction is dominated by surface or Fresnel reflections and therefore mixes linearly. Since volume scattering is a significant factor only at the smallest particle sizes, the composite spectrum radiated from a mixed surface behaves in a "checkerboard-mixing" fashion. In other words, the detected energy is a function of the areal percentage of the end-members present. Photons tend to interact once after being emitted/reflected from particles and therefore contain information only about that particular particle, or they are absorbed after being scattered, never reaching the detector.

2.2 LINEAR RETRIEVAL ALGORITHM

The fundamental principle of linear mixing is that the spectral features of the end-member minerals overlap and combine in the composite spectrum in proportion to their areal fractions. This allows for a relatively simple statistical determination of the best-fit end-member percentages for a given mixed spectrum (Adams et al., 1989). Assuming η isothermal end-members, the mathematical expression for the mixed spectrum is stated by equation (2) with the constraint that the fractions must sum to unity,

$$\varepsilon(\lambda)_{mix} = \sum_{i=1}^{\eta} \zeta_i \, \varepsilon(\lambda)_i + \delta(\lambda) ; \qquad \sum_{i=1}^{\eta} \zeta_i = 1.0 \tag{2}$$

where, ζ_i is the fractional percentage of the i^{th} end-member and $\delta(\lambda)$ is the residual error term. The residual error is calculated by subtracting the model-predicted emissivity from the measured emissivity at each wavelength. This error or mean difference of the two spectra becomes a critical measure of the retrieval algorithm's fit when displayed versus wavelength, or in image format in the case of remotely gathered data (Gillespie et al., 1990). High residual errors at specific bands indicate the possibility of an unmodeled spectral feature not present in either the end-member or mixed spectra. An examination of residuals may also reveal nonlinear behavior at certain wavelengths as well as highlight areas of poor atmospheric correction and low instrument SNR. The residual, expressed as a singular value for the entire wavelength region, is known as the root-mean-squared (RMS) error. This term determines the "goodness of fit" for that particular iteration and is related to the residual error term through the following equation,

$$RMS = \left(\sum_{j=1}^{\lambda} \delta(\lambda)_j^2 \, / \, \eta \right)^{\frac{1}{2}} \tag{3}$$

Equation 2 is typically highly overdetermined, having several unknowns (the end-member fractions and sample temperature) and 6 to several hundred equations (the radiance measured at each wavelength by the TIMS and laboratory spectrometer respectively). In order to solve the series of equations, the approach chosen was a numerical least-squares fit using a Chi-squared minimization. This methodology allows a maximum number of end-members equal to one plus the total number of equations or instrument wavelengths (Adams et al., 1986; Sabol et al., 1992). However, because one degree of freedom is removed through the assumption of an emissivity during the temperature separation, $[\zeta]$ becomes a column vector of length η. In thermal infrared images most geologic processes, such as sediment mixing along an alluvial fan or within a dune field, are easily modeled with no more than 3 or 4 end-members (Gillespie, 1992; Ramsey et al., 1994). In addition, typical rocks will not have greater than this number of minerals in abundance. Because of the mathematics involved, the least-squares algorithm can produce negative as well as positive values. Two constraints must be placed on the above methodology to produce results that are physically meaningful. First, if one or more of the final percentage values are negative, it is presumed that that end-member is not present in the mixed spectrum and is therefore removed. Second, the elements of the column vector must sum to unity.

3.0 EXPERIMENTAL PROCEDURE

3.1 LABORATORY ANALYSIS

Spectra of the mineral end-members and subsequent mixtures were either obtained from crushed, sieved, and cleaned samples with well-documented petrology or culled from the TES spectral library. Size sorting of the particles involved using a rototap sieve or a Stokes settling technique to separate the grains depending on the desired size fraction. For all experiments in this study except one, the 250-500 µm size fraction was used for spectral acquisition and mixture construction.

Thermal infrared spectra for the mineral samples were acquired in emission using a Mattson Cygnus 100 interferometric spectrometer and the one-temperature method of Christensen and Harrison (1992). The spectral wavelength region sampled is from approximately 7.1 to 25 micrometers (1400-400 cm^{-1}) which includes the diagnostic vibrational features of most rock-forming minerals. The instrument has a spectral resolution of 2 cm^{-1}

over the entire wavelength region with a SNR ratio approaching 500. Atmospheric interference due to water vapor at wavelengths short of 8 μm and carbon dioxide at wavelengths long of 12 μm is minimized by a constant nitrogen purge of the spectrometer and sample chamber. In studies of the Mattson spectrometer and the various methods of deriving emissivity, Ruff et al. (1996) have performed a detailed error analysis for all contributing factors and report an instrument precision, and thus an overall spectral reproducibility, of 0.5%.

3.2 IMAGE ANALYSIS

3.2.1 Meteor Crater, Arizona

The choice of Meteor Crater, Arizona as a test locale for the retrieval algorithm was based primarily on site's geology and lithologic diversity, therefore providing an excellent location to test the concept of linear spectral unmixing using image end-members. In addition, in recent years new scientific investigations of Meteor Crater's ejecta blanket (Grant and Schultz, 1993) have raised new questions into the amount and style of erosion that has taken place. Their findings have resulted in a much lower total vertical erosion (~ 1-2 m) than previous investigators (Shoemaker and Kieffer, 1974) who have proposed amounts as great as 20-30 m. Unmixing provides a powerful tool to map the areal extent of the ejecta more accurately than past attempts.

Meteor Crater is located in north-central Arizona on the southern edge of the Colorado Plateau, east of Canyon Diablo. Of the numerous, nearly horizontal sedimentary units that form the upper Colorado Plateau, the deepest sampled by the impact event was the Permian Coconino sandstone. Only the uppermost Coconino is exposed in the crater walls. Below the Coconino lies the 80 m thick Permian Kaibab Formation, which consists of fossfiliferous dolomitic limestone and minor calcareous sandstones. The Kaibab is in turn covered disconformably by a thin (~ 10 m), patchy veneer of the Moenkopi Formation. The upper Moenkopi exposed near the crater consists of dark reddish-brown fissile siltstones. These three units were used as image end-members and the ejecta deposits mapped with the unmixing images.

3.2.2 Kelso Dunes, California

The analysis of dune field formation, composition, and movement is critical for the interpretation of past climatic conditions and future desertification. This type of comprehensive study typically takes many man-years of data collection. However, with the use of remote sensing this time is limited dramatically giving the geologist a synoptic view of the region. The Kelso dune field was chosen as a test location for the retrieval algorithm using library derived end-members. In general, dunes represent an ideal test location as typical complications for the model such as vegetation, particle size, and subpixel thermal shadowing are minimized.

The dunes lie in the eastern Mojave Desert, California approximately 95 km west of the Colorado River and are contained within a topographic basin bounded by the Providence, Granite, Bristol and Kelso Mountains to the east, south, west and north, respectively. Previous studies have estimated the dunes range from 70% to 90% quartz mainly derived from a source 40 km to the west (Sharp, 1966; Paisely et al., 1991). In order to verify the results derived from the image analysis, 48 bulk samples were collected. Thirteen of the 48 were chosen for thin section in order to determine modal abundances, particle diameters and morphology. These samples show clear mineralogic variations throughout the dune field and contain significantly less quartz (40-50%) than previous work. The four primary mineral compositions determined from the analysis were quartz, microcline, plagioclase and magnetite. The spectra of these minerals were taken from the TES spectral library and used as end-members for the unmixing model.

3.2.3 Medicine Lake Volcano, California

Emission from lava surfaces is complicated by the presence of a glassy groundmass and/or coating. A glass by definition contains no crystalline long range order and hence is, to some degree, amorphous. This effect is evidenced when comparing the spectrum of an aphyric obsidian to a compositionally-similar crystalline rock. Changes in band morphology from vitrification and vesiculation (Ondrusek et al., 1993) could incorrectly be interpreted as changes in mineralogy. An understanding of this effect is important for accurate interpretation of remote sensing data of glassy volcanic flows and domes such as those found at Medicine Lake volcanic region in northern California. Monitoring changes in dome composition, morphology, and texture at active centers will be significant in assessing the potential eruptive state of a volcano.

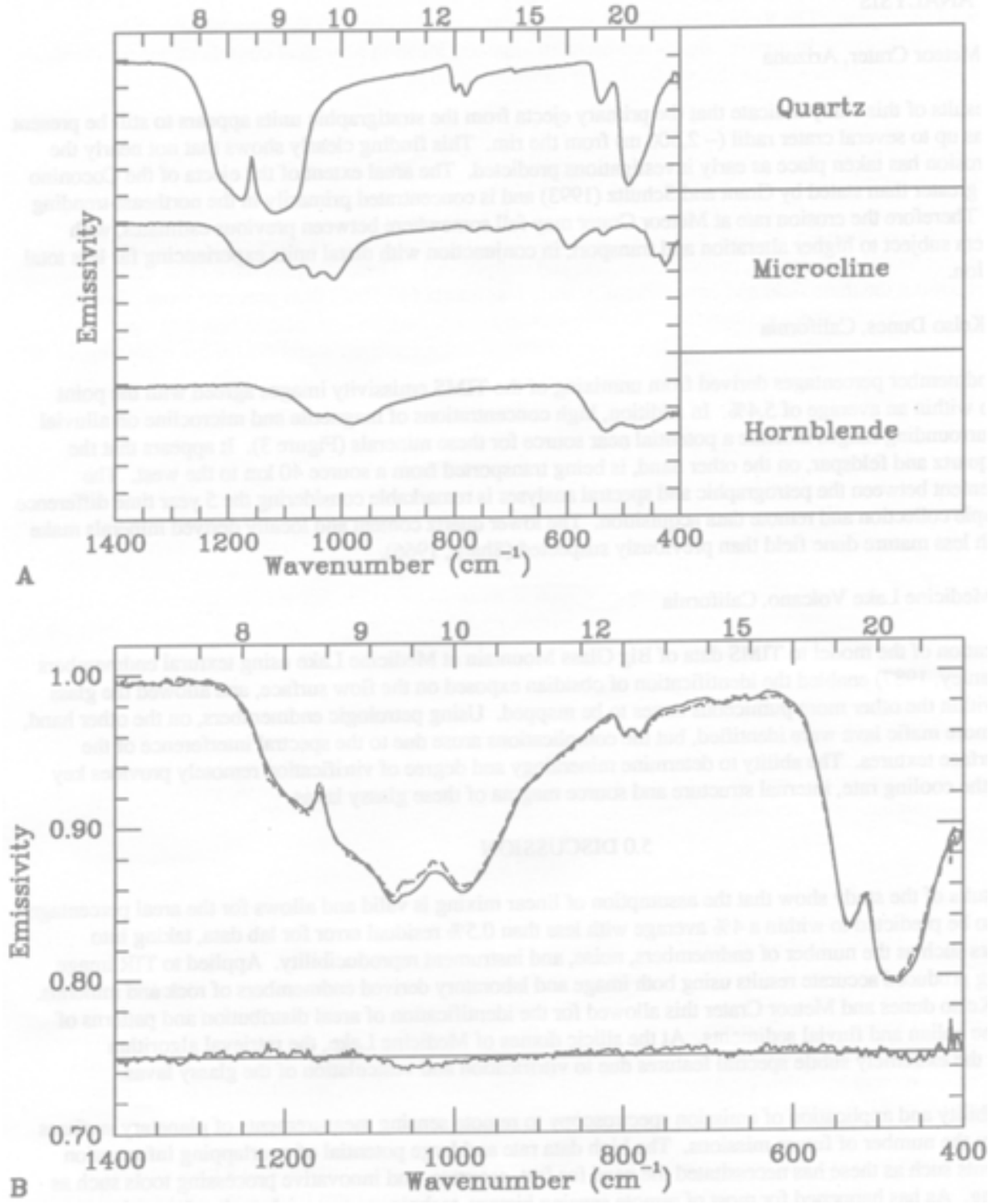

Figure 2. *(a)* Emissivity spectra of the end-members used in the 3-component mixtures of hornblende/microcline/quartz. Each tick mark represents 0.10 emissivity. *(b)* Emission spectra and retrieval model results for the 70:10:20 end-member mixture. The solid line represents the measured spectrum and the dashed, the best model fit. The residual error, shown below the spectra, has the greatest deviation over the large absorption bands and in the regions of atmospheric interference. The RMS error for this fit was 3.2×10^{-3}.

Big Glass Mountain rhyolite/dacite dome was used because of the variations in chemistry and surface textures. Located 50 km east of Mt. Shasta, the Medicine Lake highland is a low-aspect shield volcano and lies in an extensional regime with associated bimodal volcanism. The most recent activity (~ 1100 years BP) consists of silicic flows and domes ranging from dacite to rhyolite. These domes contain a wide range of pumiceous textures resulting from a combination of degassing, flow, and lava cooling (Fink and Manley, 1987).

4.0 RESULTS

4.1 LABORATORY ANALYSIS

Approximately 100 hundred mixtures of various compositions and number of end-members were constructed. For the 3-end-member suite, hornblende/microcline/quartz were used to produce several mixtures (Figure 2a). Application of the retrieval model yielded percentage errors ranging from 0.3% to 10.1% with an average of 3.6% and a RMS error of 0.38%. Figure 2 shows the model fit for the 70:10:20 mixture of hornblende/microcline/quartz respectively. The largest residual error occurs at 1000 cm^{-1} (10 μm), and corresponds to the maximum spectral contrast between quartz and hornblende. Averaged residuals for the entire spectrum are <0.5% for both mixtures indicating the validity of linear mixing.

The introduction of noise was accomplished by generating a random noise pattern with a total emissivity variation of ± 1%. This noise spectrum was then added to the spectra of the mixtures translating into a lowering of the spectrometer SNR from 500 to 200. The new "noisy" spectra were then unmixed using their original end-members. This approach is similar to Sabol et al., (1992), who examined the effects of noise on existing VNIR instruments. Decreasing the SNR produced variations in the predicted end-member percentages from a minimum of 0.6% to a maximum of 11.8%. However, the average error was only 1.98% for a >50% decrease in SNR.

4.2 IMAGE ANALYSIS

4.2.1 Meteor Crater, Arizona

The results of this study indicate that the primary ejecta from the stratigraphic units appears to still be present in many areas up to several crater radii (~ 2,500 m) from the rim. This finding clearly shows that not nearly the amount of erosion has taken place as early investigations predicted. The areal extent of the ejecta of the Coconino sandstone is greater than stated by Grant and Schultz (1993) and is concentrated primarily in the northeast-trending windstreak. Therefore the erosion rate at Meteor Crater may fall somewhere between previous estimates, with near-rim ejecta subject to higher alteration and transport, in conjunction with distal units experiencing far less total vertical erosion.

4.2.2 Kelso Dunes, California

The end-member percentages derived from unmixing of the TIMS emissivity images agreed with the point count data to within an average of 5.4%. In addition, high concentrations of magnetite and microcline on alluvial fans of the surrounding ranges indicate a potential near source for these minerals (Figure 3). It appears that the majority of quartz and feldspar, on the other hand, is being transported from a source 40 km to the west. The general agreement between the petrographic and spectral analyses is remarkable considering the 5 year time difference between sample collection and remote data acquisition. The lower quartz content and locally derived minerals make Kelso a much less mature dune field than previously suspected (Sharp, 1966).

4.2.3 Medicine Lake Volcano, California

Application of the model to TIMS data of Big Glass Mountain at Medicine Lake using textural end-members (Fink and Manley, 1987) enabled the identification of obsidian exposed on the flow surface, and allowed the glass percentage within the other more pumiceous zones to be mapped. Using petrologic end-members, on the other hand, locations of more mafic lava were identified, but the complications arose due to the spectral interference of the overriding surface textures. The ability to determine mineralogy and degree of vitrification remotely provides key insights into the cooling rate, internal structure and source magma of these glassy lavas.

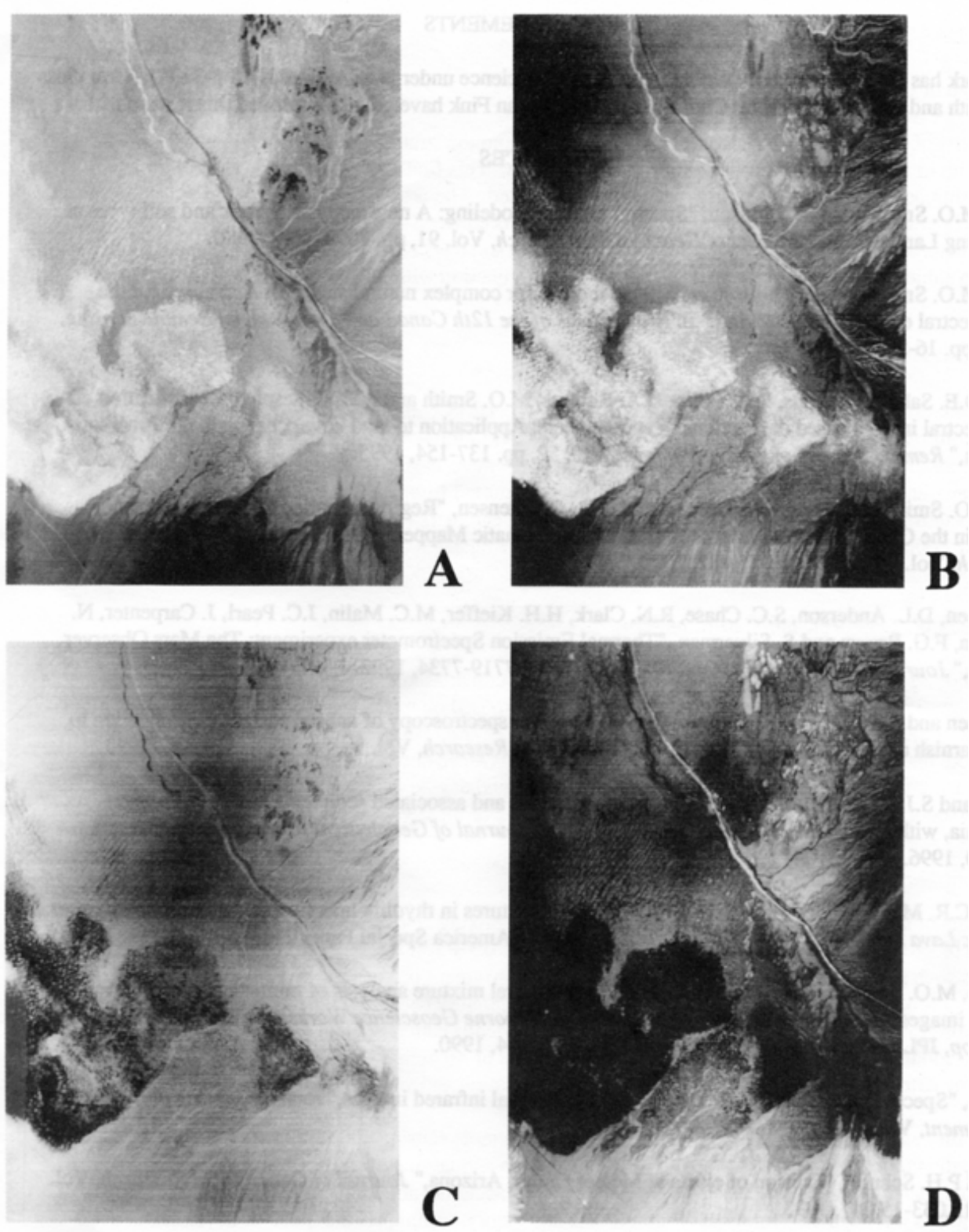

Figure 3. Model results for TIMS imagery of the Kelso dune field, Mojave Desert, California. The scene was modeled with four laboratory mineral end-members – quartz, microcline, oligoclase, and magnetite. Comparisons of predicted end-member percentages with point counts from field samples shows an average model difference of 5.4% with a RMS of 1.36×10^{-3}. *(a)* Quartz end-member. *(b)* Microcline end-member. *(c)* Plagioclase end-member. *(d)* Magnetite/clay end-member.

5.0 DISCUSSION

The results of the study show that the assumption of linear mixing is valid and allows for the areal percentage of a mineral to be predicted to within a 4% average with less than 0.5% residual error for lab data, taking into account factors such as the number of end-members, noise, and instrument reproducibility. Applied to TIR image data, unmixing produced accurate results using both image and laboratory derived end-members of rock and minerals. For both the Kelso dunes and Meteor Crater this allowed for the identification of areal distribution and patterns of transport of the eolian and fluvial sediments. At the silicic domes of Medicine Lake, the retrieval algorithm discriminated the extremely subtle spectral features due to vitrification and vesiculation of the glassy lavas.

The viability and application of emission spectroscopy to remote sensing measurements of planetary surfaces is evident from the number of future missions. The high data rate and large potential of overlapping information from instruments such as these has necessitated the need for fast, accurate, and innovative processing tools such as linear unmixing. As has happened for most of remote sensing history, techniques are quick to develop and even quicker to be discarded as the next innovation is unveiled. It is critical, however, to understand the physics of thermal emission and how it is effected by more complex problems such as the mixing of radiant energy. Such an understanding in conjunction with the use of a linear retrieval approach and well-defined spectral mineral library will allow for a quick, modal analysis in the laboratory. In addition, it provides an excellent method of reducing hyperspectral, remotely gathered data to manageable sets of surface end-member (mineral) maps.

6.0 ACKNOWLEDGEMENTS

This work has been supported by funding from ASTER science under NASA grant NAS 5-31371. Countless discussions with and advice from Philip Christensen and Jonathan Fink have greatly improved this research.

7.0 REFERENCES

J.B. Adams, M.O. Smith and P.E. Johnson, "Spectral mixture modeling: A new analysis of rock and soil types at the Viking Lander I site," *Journal of Geophysical Research,* Vol. 91, pp. 8098-8112, 1986.

J.B. Adams, M.O. Smith and A.R. Gillespie, "Simple models for complex natural surfaces: A strategy for the hyperspectral era of remote sensing." In *Proceedings of the 12th Canadian Symposium on Remote Sensing,* Vol. 1, pp. 16-21, July 1989.

J.B. Adams, D.E. Sabol, V. Kapos, R.A. Filho, D.A. Roberts, M.O. Smith and A.R. Gillespie, "Classification of multispectral images based on fractions of end-members: Application to land-cover change in the Brazilian Amazon," *Remote Sensing of the Environment,* Vol. 52, pp. 137-154, 1995.

G. Blount, M.O. Smith, J.B. Adams, R. Greeley and P. R. Christensen, "Regional aeolian dynamics and sand mixing in the Gran Desierto: Evidence from Landsat Thematic Mapper images," *Journal of Geophysical Research,* Vol. 95, pp. 15,463-15,482, 1990.

P.R. Christensen, D.L. Anderson, S.C. Chase, R.N. Clark, H.H. Kieffer, M.C. Malin, J.C. Pearl, J. Carpenter, N. Bandeira, F.G. Brown and S. Silverman, "Thermal Emission Spectrometer experiment: The Mars Observer Mission," *Journal of Geophysical Research,* Vol. 97, pp. 7719-7734, 1992.

P.R. Christensen and S.T. Harrison, "Thermal-infrared emission spectroscopy of natural surfaces: Application to desert varnish coatings on rocks," *Journal of Geophysical Research,* Vol. 98, pp. 19,819-19,834, 1993.

J.K. Crowley and S.J. Hook, "Mapping playa evaporite minerals and associated sediments in Death Valley, California, with multispectral thermal infrared images," *Journal of Geophysical Research,* Vol. 101, pp. 643-660, 1996.

J.H. Fink and C.R. Manley, "Origin of pumiceous and glassy textures in rhyolite lava flows." In *The Emplacement of Silicic Lava Domes and Flows,* Geologiocal Society of America Special Paper 212, pp. 77-88, 1987.

A.R. Gillespie, M.O. Smith, J.B. Adams and S.C. Willis, "Spectral mixture analysis of multispectral thermal infrared images." In *Summaries of the Second Annual Airborne Geoscience Workshop, Vol. 2, TIMS Workshop,* JPL Publication 90-55, Pasadena, Ca., pp. 57-74, 1990.

A.R. Gillespie, "Spectral mixture analysis of multispectral thermal infrared images," *Remote Sensing of the Environment,* Vol. 42, pp. 137-145, 1992.

J.A. Grant and P.H. Schultz, "Erosion of ejecta at Meteor Crater, Arizona," *Journal of Geophysical Research,* Vol. 98, pp. 15,033-15,047, 1993.

P.E. Johnson, M.O. Smith, S. Taylor-George and J.B. Adams, "A semiempirical method for analysis of the reflectance spectra of binary mineral mixtures," *Journal of Geophysical Research,* Vol. 88, pp. 3557-3561, 1983.

A.B. Kahle, and A.F.H. Goetz, "Mineralogic information from a new airborne thermal infrared multispectral scanner," *Science,* Vol. 222, pp. 24-27, 1983.

A.B. Kahle, F.D. Palluconi, S.J. Hook, V.J. Realmuto and G. Bothwell, "The advanced spaceborne thermal emission and reflectance radiometer (ASTER)," *International Journal of Imaging Systems and Technology,* Vol. 3, pp. 144-156, 1991.

R.J.P. Lyon, *Evaluation of infrared spectrophotometry for compositional analysis of lunar and planetary soils, Part II: Rough and powdered surfaces,* Stanford Research Institute, NASA-CR-100, Washington, D.C., 1964.

J. Ondrusek, P.R. Christensen and J.H. Fink, "Mapping the distribution of vesicular textures on silicic lavas using the Thermal Infrared Multispectral Scanner,", *Journal of Geophysical Research,* Vol. 98, pp. 15,903-15,908, 1993.

E.C.I. Paisley, N. Lancaster, L.R. Gaddis and R. Greeley, "Discrimination of Active and Inactive Sand from Remote Sensing: Kelso Dunes, Mojave Desert, California," *Remote Sensing of the Environment,* Vol. 37, pp. 153-166, 1991.

F.D. Palluconi and G.R. Meeks, *Thermal infrared multispectral scanner (TIMS): An investigators guide to TIMS data,* JPL Publication 85-32, Pasadena, Ca., p. 14, 1985.

M.S. Ramsey, D.A. Howard, P.R. Christensen and N. Lancaster, "Sand sources and mineralogic variability within the Kelso Dune field, Mojave Desert, California: Analysis of thermal infrared remote sensing data," In *Geological Society of America Abstracts with Programs,* Vol. 26, p. A-89, 1994.

S. Ruff, P.R. Christensen, P.W. Barbera and D.L. Anderson, "Quantitative thermal emission spectroscopy of minerals: A technique for measurement and calibration," to be submitted to *Journal of Geophysical Research,* 1996.

D.E. Sabol, J.B. Adams and M.O. Smith, "Quantitative subpixel spectral detection of targets in multispectral images," *Journal of Geophysical Research,* Vol. 97, pp. 2659-2672, 1992.

J.W. Salisbury and L.S. Walter, "Thermal infrared (2.5-13.5 μm) spectroscopic remote sensing of igneous rock types on particulate planetary surfaces," *Journal of Geophysical Research,* Vol. 94, pp. 9192-9202, 1989.

R.P. Sharp, "Kelso Dunes, Mojave Desert, California," *Geological Society of America Bulletin,* Vol. 77, pp. 1045-1074, 1966.

E.M. Shoemaker and S.W. Kieffer, *Guidebook to the geology of Meteor Crater, Arizona,* Arizona State University Center for Meteorite Studies, Publication 17, Tempe, Az., pp. 66, 1974.

R.B. Singer, and T.B. McCord, "Mars: Large scale mixing of bright and dark surface materials and implications for analysis of spectral reflectance," In *Proceedings of the Lunar and Planetary Science Conference XX,* pp. 1835-1848, 1979.

J.L. Thomson and J.W. Salisbury, "The mid-infrared reflectance of mineral mixtures (7-14 μm)," *Remote Sensing of the Environment,* Vol. 45, pp. 1-13, 1993.